Sound and vibration transmission through lightweight junctions: Numerical investigation and validation by laboratory tests.

S. Lentzen, E. Gerretsen, C. van Bentum, S. Bron-van der Jagt
TNO Built Environment and Geosciences, The Netherlands

Introduction

Lightweight building concepts are gaining increasing interest amongst architects, engineers and manufactures due to several advantages. Obviously, lightweight concepts can offer a sustainable solution in several ways. The amount of required resources is smaller compared to traditional concepts and materials can optionally be re-used. Transportation costs and building times are reduced. Adjustment of existing dwelling is more easily adopted to the changing needs.
However, an important issue that has to be dealt with is the sound and vibration insulation. Due to increasing comfort expectations of inhabitants and the inability to accurately predict the insulation capabilities, building companies seem be reluctant towards using lightweight concepts.
An important parameter used for predicting the sound insulation between rooms is the vibration reduction index K_{ij} [1, 2] describing the insulation properties of a building junction. Models predicting K_{ij} are well established for heavy, monolithic junction. Lightweight juntions generally require more complicated designs involving several transmission paths. Therefore at present the existing models cannot generally be applied to lightweight junctions.
Another aspect that plays an important role is low frequency or walking induced vibration. Sound insulators operate in a different frequency range than the vibration frequencies which are induced by walking and vice versa. Therefore both aspects can have a "competitive relationship".
In this work the sound and vibration characteristics of several lightweight junctions are numerically investigated with FEM (for the low- and the mid-frequency range) and SEA (for the mid- and the high-frequency range). In order to validate these analyses, the junctions are tested in a laboratory setting. For sound insulation the investigations are focused on obtaining the vibration reduction indices K_{ij}. These are not only investigated for the floor-floor flanking transmission path, but also for all the other possible paths (e.g. floor-wall, floor-ceiling and wall-ceiling).
Looking at the vibration behaviour and transmission, the main focus was put on obtaining the One-Step-RMS velocities of the floors. In these investigations the point- and transfermobilities are acquired either by numerical analyses or by measurements. Since these spectra are only required for frequencies up to 40Hz, the numerical study consists merely of FEM analysis.

Experimental setup

In total six variants of junctions have been studied at the building laboratory of TNO. Figure 1 shows the experimental setup en Figure 2 shows a schematic representation of the six variants. The steel supporting

Figure 1: The experimental setup at the TNO building laboratory.

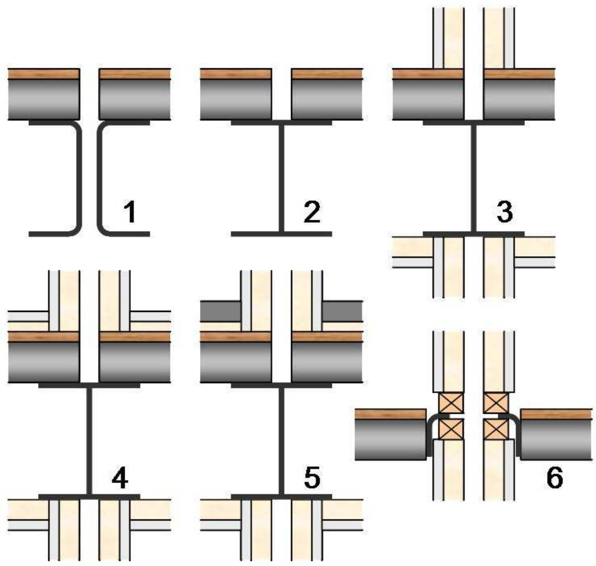

Figure 2: The six variants of junctions which are studied.

frame consists of beams and columns. At the junction two HEA 240 columns, which are separated by 5 m, are supporting either two UNP 200 beams (variant 1) or one HEA 240 beam (variant 2). The floors (5 m × 5 m) are supported by the beams. They consist of equidistantly distributed (400 mm) light steel C-profiles (height 185 mm) with a 20 mm thick wooden plate screwed on top of it. Both variants also exist with a

flexible Sylomer layer in between the beams and the floor, which is denoted as the variants 1a and 2a.
In variant 3 the walls and ceilings are added. These consist of gypsum plates screwed on C-profiles (wall: 2× Gyproc 12.5 mm with 160 mm cavity, ceiling: 2× Gyproc RF 12.5 mm with 80 mm cavity). The cavities are filled with mineral wool. In variant 4 gypsum plates (2× Gyproc RF 10 mm) on top of 20 mm thick mineral wool are added to the floor. In variant 5 this gypsum plate floor is replaced with an anhydrite floor poured over a dovetailed steel sheet. The steel sheet is elastically supported by 17 mm thick equidistantly ditributed (400 mm) rubber strips.
The sixth variant is fundamentally different from the previous five. In this variant the overall structural integrity is also provided by the walls and the floors. The floor elements are similar to those used in variant 3. They are supported by the walls. These walls are indirectly connected to each other by the aformentioned HEA 240 columns.

Vibration level differences ΔL_v and vibration reduction indices K_{ij} between the floors, the walls and the ceilings have been determined according to ISO 10848 [3]. The floors are excited with the ISO-hammer box [4] and the remaining elements with an hammer. The response of each element has been measured with 6 to 10 accelerometers.
The vibration levels caused by walking at the emitting and the receiving floor have been predicted according to a Dutch standard [5] which provides the basis for a European standard under development. With the method described in [5], velocity levels caused by one step (OS-RMS-values) are predicted for walking loads corresponding to various walking frequencies and masses of the walking person. The used load spectra are defined in the standard. These spectra are projected on the transfer mobilities for all combinations of excitation and response points considered during the measurements. From all OS-RMS-values determined according to this procedure at one point, the 90% upper level (OS-RMS90) is determined. These levels are averaged over each floor. In order to obtain the transfer mobilities between the floors an impact hammer is used to excite them and the velocity spectra are determined using accelerometers.

Numerical investigation

The vibration reduction index K_{ij} is used to qualify the noise attenuation in a building junction for the path starting at component i and ending at component j. In case the elements are lightweight, it can be expressed as

$$K_{ij} = \frac{\Delta L_{v,ij} + \Delta L_{v,ji}}{2} + 10 \lg \frac{\ell_{ij}}{\sqrt{S_i S_j}}, \quad \text{[dB]} \qquad (1)$$

where $\Delta L_{v,ij}$ is the difference in velocity level between the component i and j, where component i is excited. The length of the building junction is denoted by ℓ_{ij} and S_i denotes the surface area of component i. It is thus sufficient to compare the measured differences in velocity levels to the predicted differences.
Figure 3 displays the geometry of the FEM-model of the third variant. The model consists of up to 250 thousand

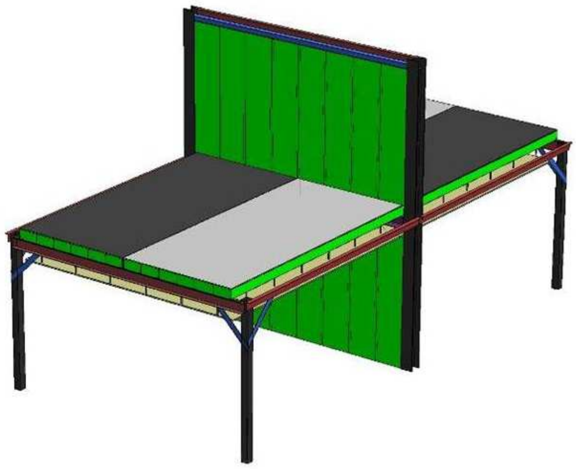

Figure 3: The FEM model of variant 3.

shell and solid elements. The size of these elements is chosen as one sixth of the flexural wave length at 250 Hz. The analysis is performed in the frequency domain and takes up to four days for all excitations of one variant. The applied material parameters are displayed in Table 1, where ζ is the damping factor modelled with Rayleigh damping.

Material	Parameter			
	E [kN/mm^2]	ρ [kg/m^3]	ν [-]	ζ [-]
Steel	182	7700	0.3	0.001
Gypsum	3.1	720	0.3	0.015
Reinforced gypsum	2.5	1150	0.3	0.02
Wood	4.2	480	0.3	0.02
Anhydrite	15	2050	0.15	0.01
Rubber	0.0015	600	0.2	0.1
Sylomer	0.0003	300	0.2	0.1

Table 1: Material parameters.

Figure 4 displays the SEA model of the third variant. SEA has only been applied to model the sound trans-

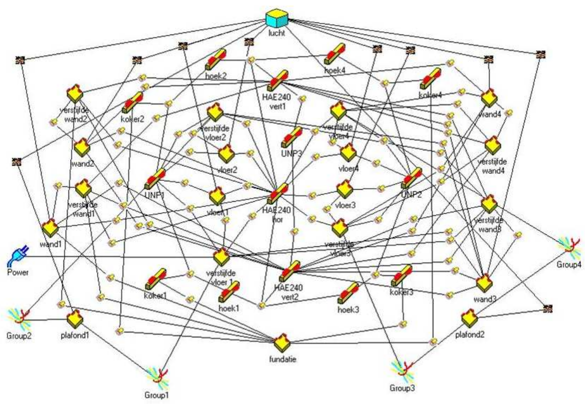

Figure 4: The SEA model of variant 3.

mission and not the walking induced vibrations. The floor and wall elements are modelled by two subsystems representing bending and compression modes. The beams and columns are modelled by three subsystems, representing bending, compression and torsion modes. The floor and wall elements are stiffened plate structures. For each plate structure, separate subsystems are used, representing the global vibrational behaviour of the entire plate structure including stiffeners (up to 1600 Hz) and the vibrational behaviour of the plate fields between the stiffeners (from 250 Hz).
The material properties, except the damping, can be found in Table 1. The stiffened floor elements (representing global vibrational behaviour), floors (representing higher order bending modes), stiffened wall elements, walls, beams and columns are assumed to have loss factors η of 2%, 1%, 4%, 4%, 2% and 1%, respectively.
The SEA models consist of up to 260 subsystems with 800 couplings. The computation times are in the order of 10 seconds for an analysis in 24 1/3 octave bands.

Results and conclusions

Figures 5 to 8 represent the quality of agreement between the measured (red curve), the FEM- (green curve) and the SEA-results (black curves).

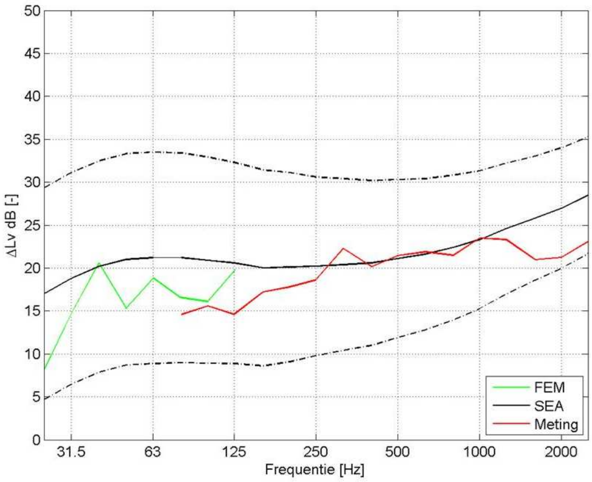

Figure 5: $\Delta L_{v,ij}$ between the floors of variant 1.

Generally the difference between the measured data and the SEA predictions is limited to 5 dB and the agreement is therefore considered good. The difference between the measurements and the FEM predictions is limited to 10 dB and therefore the FEM models require further attention. The worst agreement is obtained in the predictions of variant 1a. Both the FEM- and the SEA-analyses overpredict the vibration attentuation between the floors. This can, at least partly, be explained by the airborne sound transmission from the tapping machine, which is not simulated in the numerical models. In this variant there are no walls present to obstruct the sound field. The disagreement is not present in variant 2a, because the differences $\Delta L_{v,ij}$ are much smaller due to the absence of the dilatation in the junction.

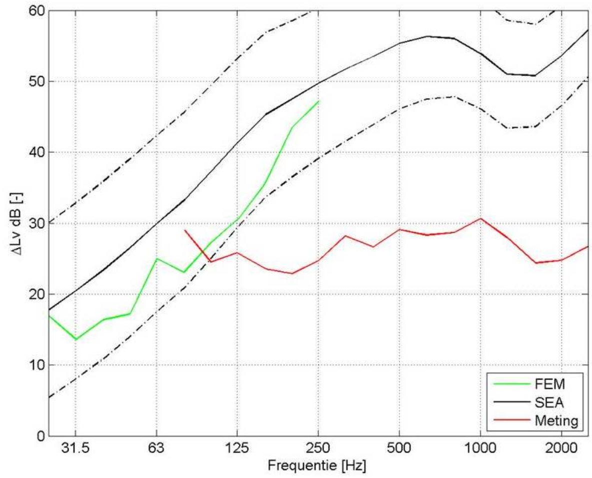

Figure 6: $\Delta L_{v,ij}$ between the floors of variant 1a.

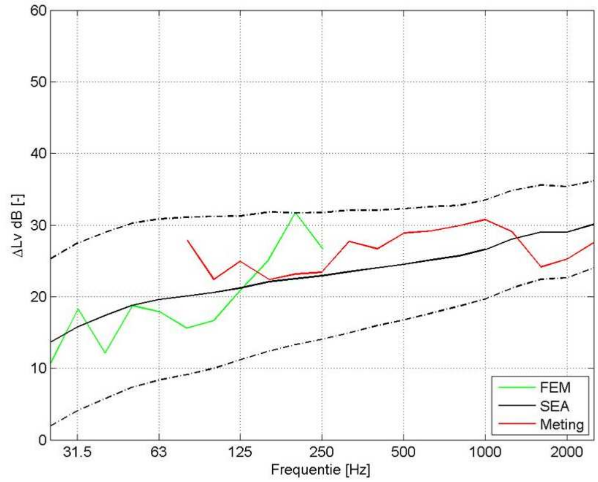

Figure 7: $\Delta L_{v,ij}$ between the floors of variant 2a.

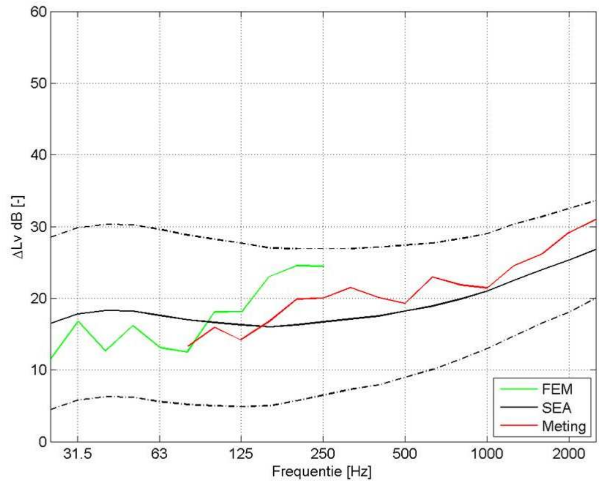

Figure 8: $\Delta L_{v,ij}$ between the floors of variant 3.

More detailed information about the measurements, the numerical analyses and the results can be found in a TNO report [6]. In this reference it can be found that the predictions of $\Delta L_{v,ij}$ for other paths also agree well with the measured data.

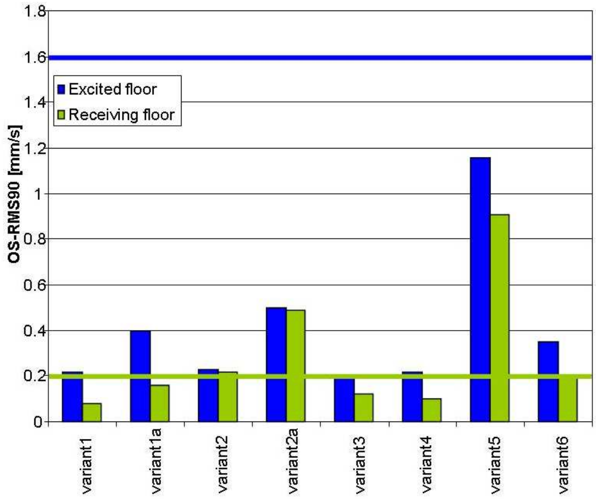

Figure 9: Measured OS-RMS90 values for the excited (blue) and the receiving (green) floor.

Figure 9 displays the resulting OS-RMS90 values of the measurements. The blue and the green line indicate the maximum levels for the excited and the receiving floor, respectively, which are considered acceptable.

From the measurements the following conclusions can be drawn. It is seen that the difference in OS-RMS90 between the excited and the receiving floor is relatively large for the variants 1 and 1a. This can be explained by the lack of coupling between both floors. The only coupling between them exists in an indirect way by the HEA 240 columns, which support the two UNP 200 beams. Variant 1a shows larger responses. This is probably due to the flexible Sylomer layers between the floors and the UNP beams. These layers work well for the sound insulation, but they seem to enhance the walking induced vibrations.

The difference in responses between both floors of the variants 2 and 2a are nearly equal. This is due to the coupling between the floors. Both floors are supported by the same HEA beam. The effect of dilatation is apparent when comparing the results of variant 1 and variant 2.

For variants 3 and 4 the overall response is lower than in the previous variants. This can be explained by the presence of the walls and the ceilings. A substantial amount of vibration energy flows into these components reducing the vibration levels of the floors. The difference between the excited and the receiving floors is not yet as large as in the uncoupled case.

The vibration levels in variant 5 are surprisingly high. Further investigations reveiled that the first eigenfrequency of the floors in this variants is present at about 5 Hz whereas the first eigenfrequency of the floor in variant 4 is present at about 12 Hz. The load spectra of one step of a walking person show a maximum at frequencies below 6 Hz. The fact that the present floors have low eigenfrequencies may be explained by the 17 mm thick rubber strips supporting the dovetailed steel sheet. A solution to this problem may be found in tuning the rubber strips such that the eigenfrequencies of the floors will increase above 10 Hz.

Until now, the walking induced vibrations have been simulated up to variant 3 and the results are displayed in Table 2. It can be noticed that the differences between

Variant	measurement		FEA	
	excited	receiving	excited	receiving
1	0.22	0.08	0.21	0.07
1a	0.4	0.16	0.97	0.61
2	0.23	0.22	0.13	0.12
2a	0.5	0.4	0.23	0.22
3	0.2	0.12	0.07	0.05

Table 2: OS-RMS90-values [mm/s]: comparison between measurements and FEA.

the excited floors and the receiving floors predicted with the FEM-models agree reasonably well with those measured. The comparison between the predicted and the measured absolute values show a relative factor of maximally 2 between both. This is reasonably good, since the OS-RMS results are very sensitive to the location of the eigenfrequencies.

References

[1] EN 12354-1, Building Acoustics - Estimation of acoustic performance of buildings from the performance of elements - Part 1: Airborne sound insulation between rooms, 2000.

[2] EN 12354-2, Building Acoustics - Estimation of acoustic performance of buildings from the performance of elements - Part 2: Impact sound insulation between rooms, 2000.

[3] ISO 10848, Acoustics - Laboratory measurement of the flanking transmission of airborne and impact noise between adjoining rooms, Part 1-4, 2005.

[4] ISO 140-6, Acoustics - Measurement of sound insulation in buildings and of building elements, Part 6: Laboratory measurements of impact sound insulation of floors, 1998.

[5] SBR richtlijn, Trillingen van vloeren door lopen - Richtlijn voor het voorspellen, meten en beoordelen, 2005.

[6] Bouwknopen in lichtgewicht gebouwen, rapportage fase 2 van het TNO-Co onderzoek, TNO report number 2008-D-R0341/B, March 2008.